Supplementary Figures

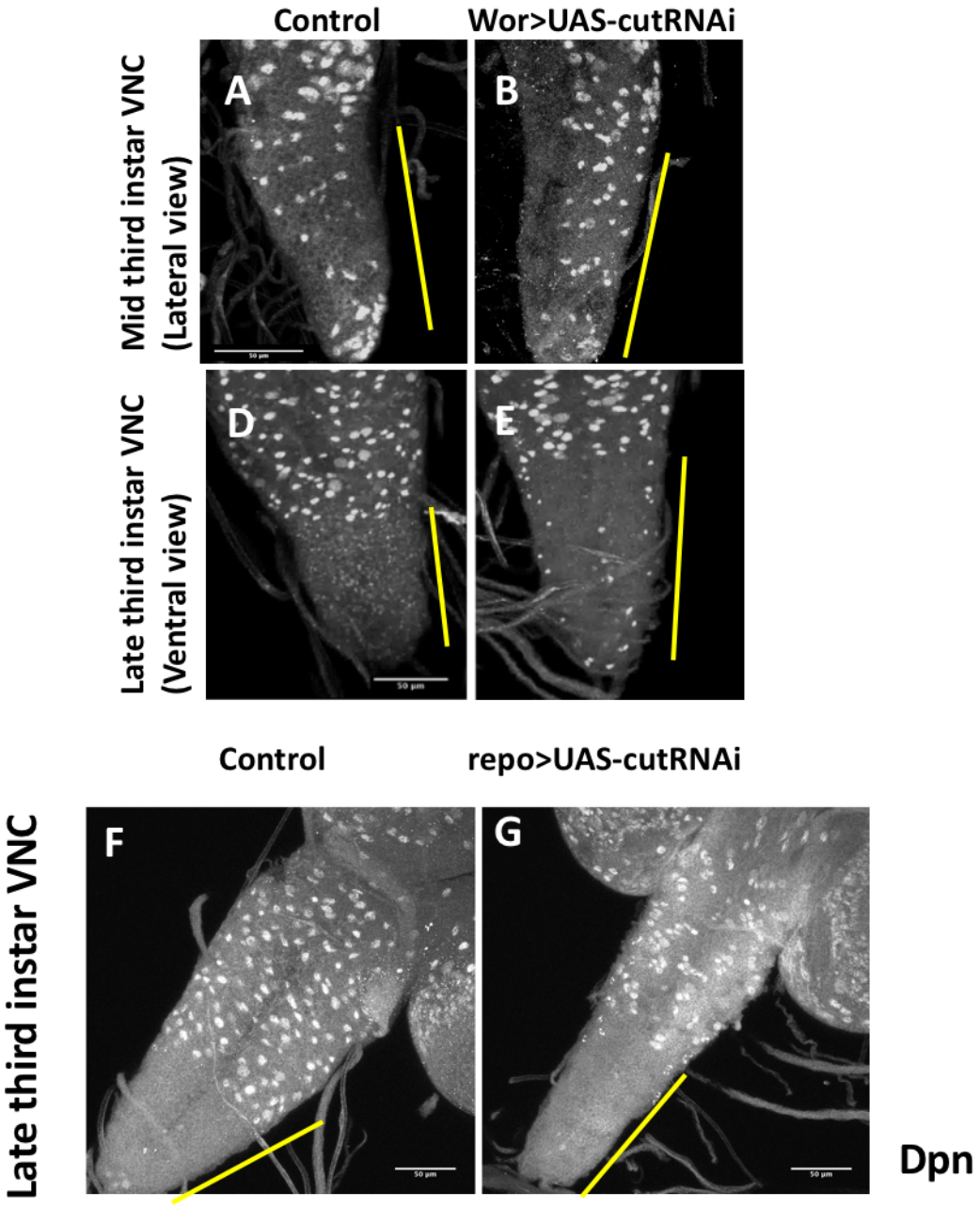

Figure S1. Knockdown of *cut* in the CNS with wor>cutRNAi results in ectopic NB survival in larvae, as visualized with anti-Dpn staining. A, B) In mid-third instar larvae, ectopic NBs are clearly visible in the abdominal ganglia (yellow bar). **C, D)** In late third instar larvae, many of these ectopic NBs have died, but at least one ectopic abdominal NB lineage remains. **F, G)** Knockdown of *cut* in glia with repo>cutRNAi does not result in ectopic NB survival. Yellow bars mark the abdominal region.

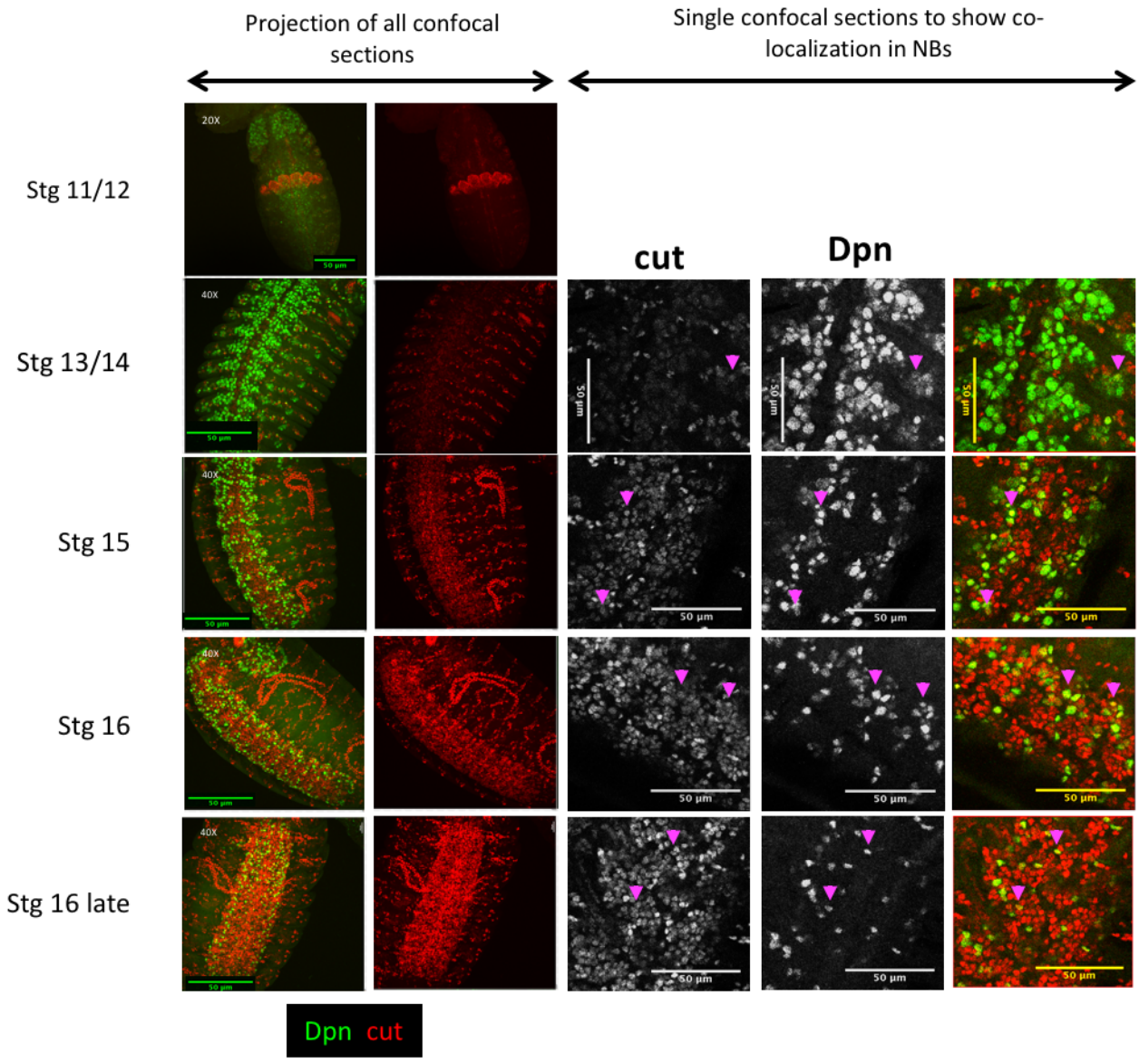

Figure S2. Cut expression in the CNS corresponds to the period of NB death. Cut levels increase in the CNS starting at stage 13/14. A small number of NBs (identified by Dpn staining) are Cut+ at this stage (pink arrowheads). Cut levels are highest by late stage 16, and many NBs are Cut positive. All embryos were imaged at the same settings for Cut staining intensity.

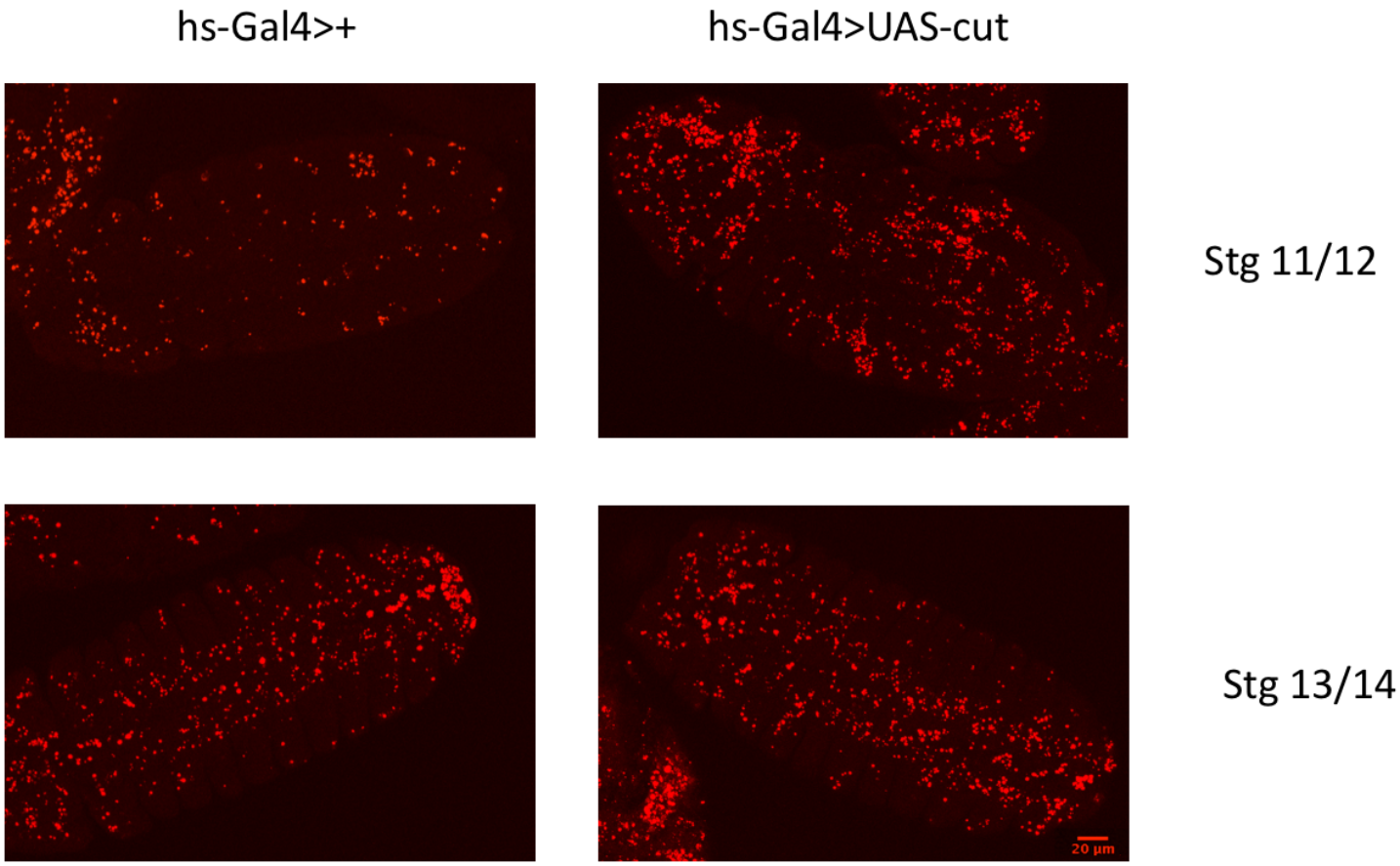

Figure S3. Expression of *cut* under control of the heat shock promoter results in a large increase in cell death, both within the nervous system and in other tissues. TUNEL staining marks apoptotic cells. An overnight collection of embryos from the cross hs-gal4 X UAS-cut mcd8GFP/Bal was heat shocked for 1.5 hours at 37o, allowed to recover for 4 hours and then stained for TUNEL and GFP, GFP staining is not shown.

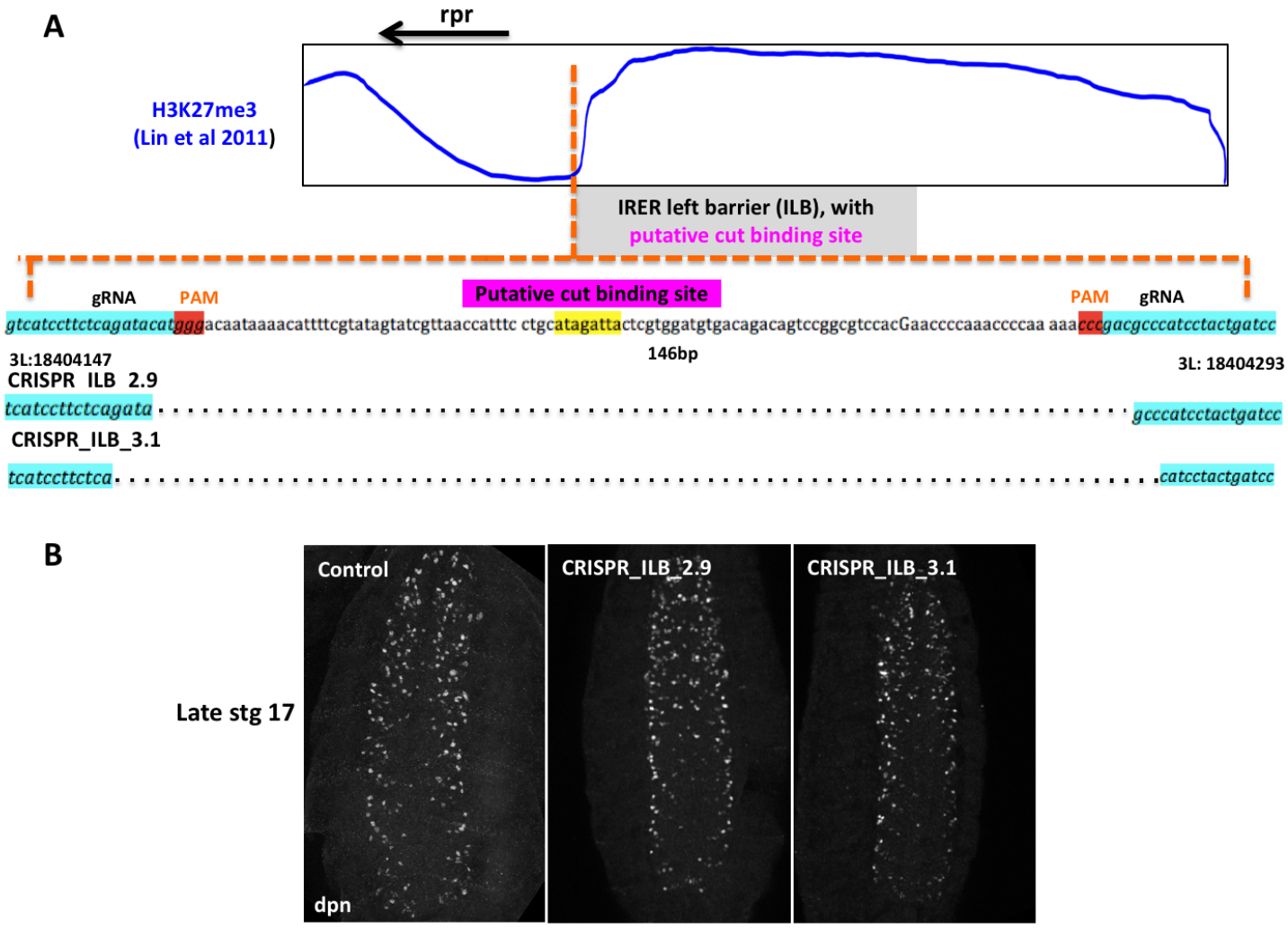

Figure S4. Crispr strategy for deletion of the putative Cut binding site at the ILB A) The reported Cut binding site lies within the IRER left boundary (ILB), marked by a sharp decrease in H3K27me3 binding 5' of the *rpr* transcribed region in S2 cells and adult flies (Lin et al., 2011). Guide RNAs for CRISPR/Cas9 were selected to flank the binding site. Transgenic gRNA flies were crossed to nos-Cas9, and screened for deletions by PCR. Breakpoints were confirmed by sequencing. **B)** Late embryos homozygous for two deletions of the Cut binding site (CRISPR_ILB_2.9 and CRISPR_ILB_3.1) do not result in ectopic NB survival.

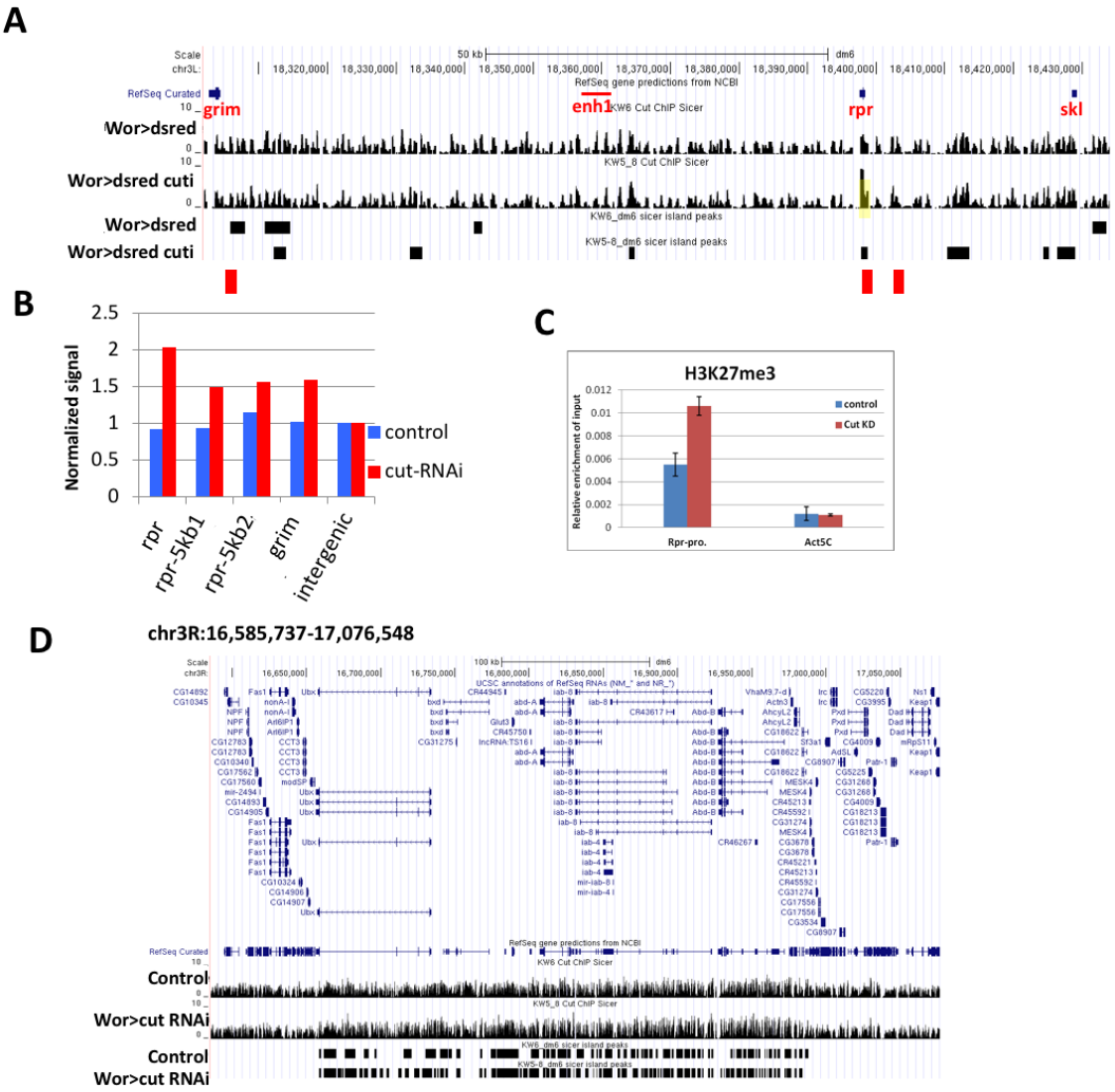

Figure S5. A) H3K27me3 ChIP-Seq on sorted CNS nuclei from wor-gal4 UAS-nls-dsRed>+ and wor-gal4 UAS-nls-dsRed >cutRNAi show a significant increase in enrichment at rpr (highlighted) and a slight increase in H3K27me3 modifications in the *rpr* region after *cut* knockdown, as detected by SICER peak calling. Primer regions used in B are boxed in red. **B)** Verification by ChIP-qPCR on independent chromatin preparations show increased enrichment of H3K27me3 at the promoters of grim and *rpr*, and 5kb 5' of *rpr* (*rpr*-5kb1&2). All data are normalized to levels in an intergenic region. Primer regions are boxed in red in A.**C)** H3K27me3 ChIP with an independent chromatin preparation from sorted nuclei demonstrates increased enrichment of H3K27me3 at the *rpr* promoter following *cut* knockdown. **D)** H3K27me3 ChIP from NB nuclei shows strong enrichment in the bithorax complex. *cut* knockdown results in a slight increase in SICER peaks in the region.

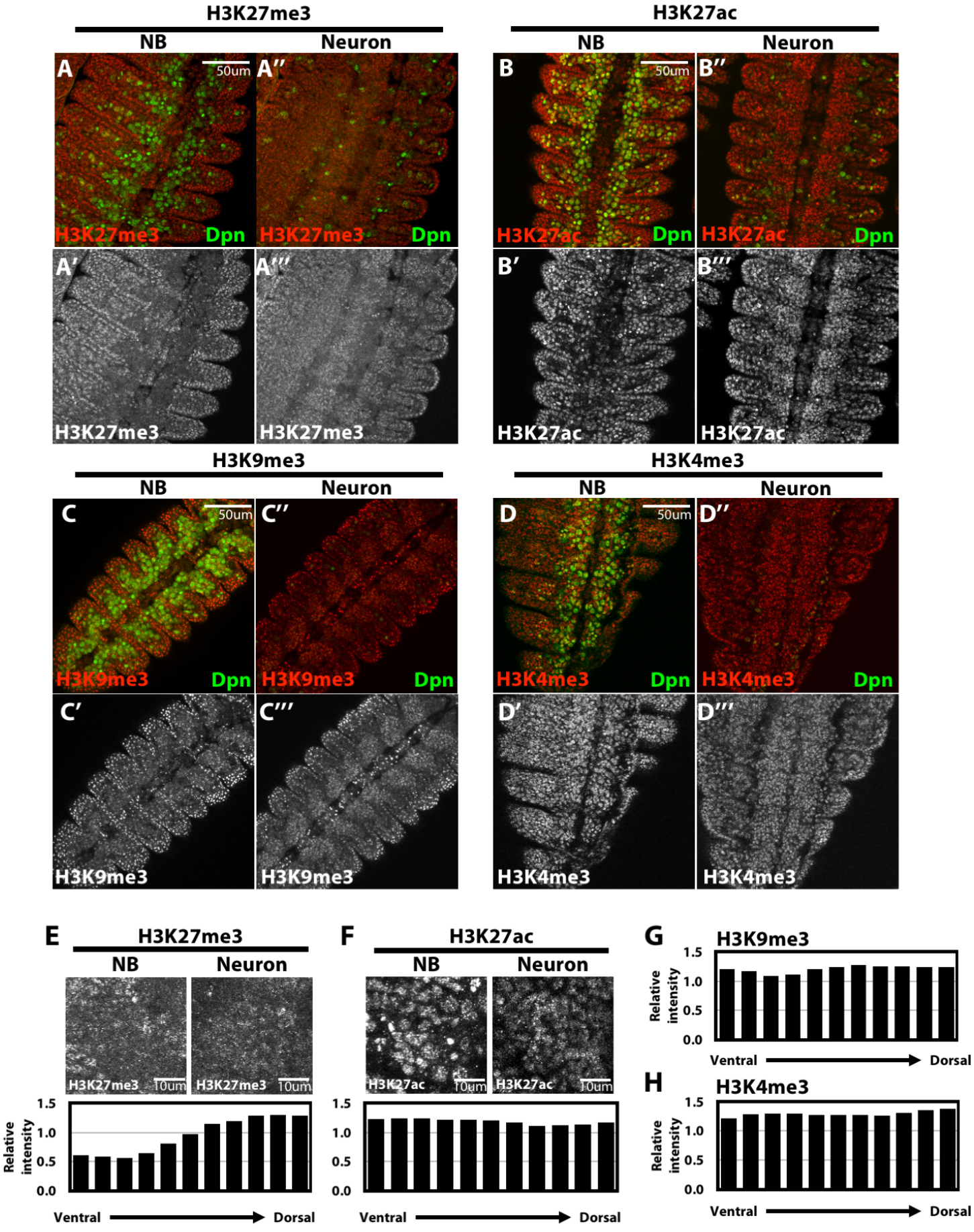

Figure S6. H3K27me3, but not other histone modifications, shows differential enrichment between neuroblast and neuron layers of the VNC of stage 13 embryos. H3K27me3 **(A-A'''')** is absent from Dpn-positive neuroblasts (**A and A'**) at this stage, but is present in dorsal layers of the nerve cord that contain neurons (**A'' and A'''**). H3K27ac (**B-B'''**), H3K9me3 (**C-C'''**) and H3K4me3 (**D-D'''**) are present in both neuroblast and neuronal layers of the VNC. Relative H3K27me3 levels increase along the ventral-dorsal axis in the VNC: H3K27me3 staining is shown within one hemisegment of the VNC at the level of neuroblasts (**E**, top left) or neurons (**E**, top right), and quantified as relative intensity within each single confocal slice, normalized to the epidermis (**E**, bottom). In contrast, there is no change in relative H3K27ac levels along the ventral-dorsal axis, as shown in one hemisegment at the level of neuroblasts (**F**, top left) or neurons (**F**, top right), and quantified as in **E** (**F**, bottom). **G)** H3K9me3 is generally lower in the VNC overall, and shows slight reduction in relative levels in NBs at this stage. There is no change in relative levels of H3K4me3 in the CNS, as shown in **H**.

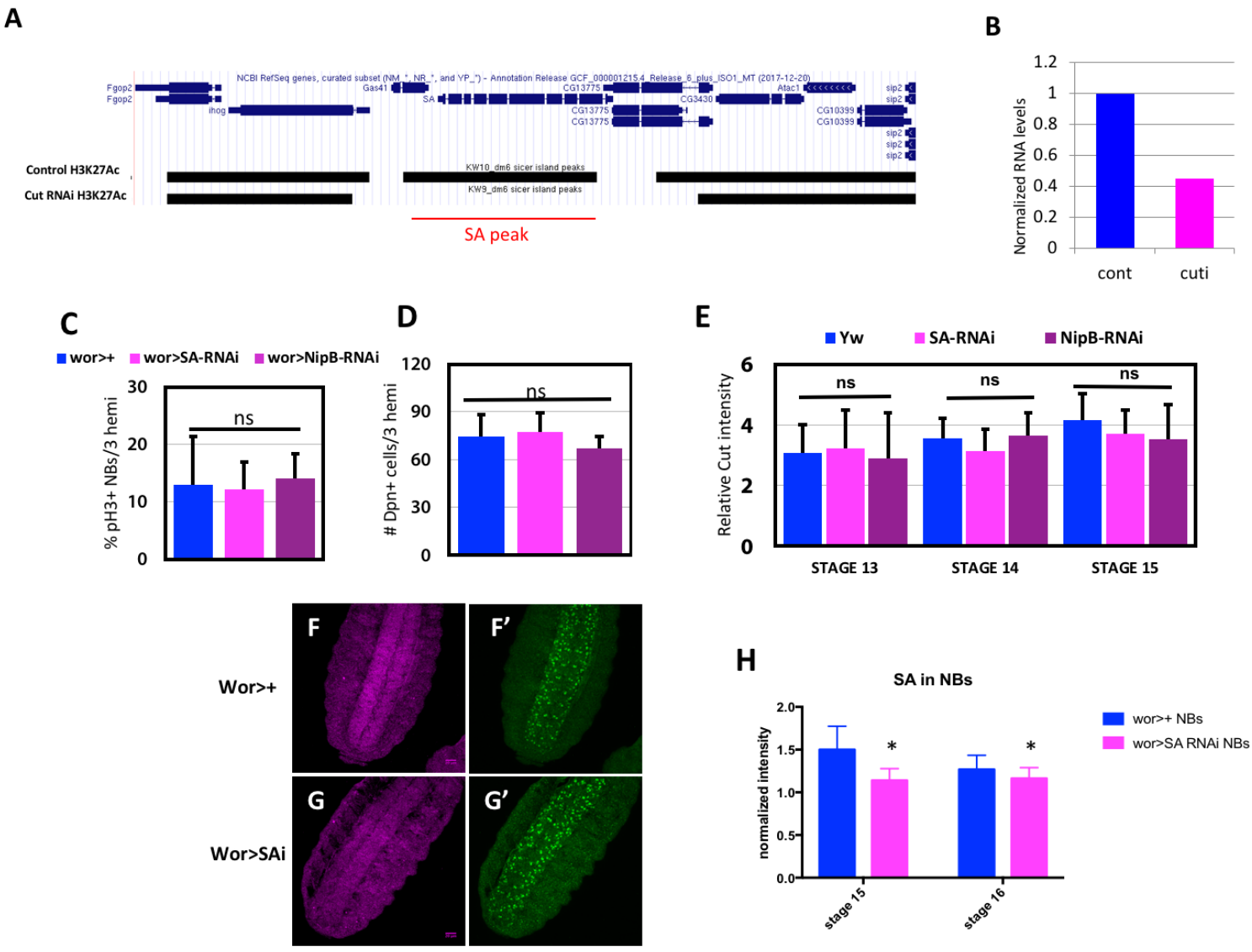

Figure S7. *SA* knockdown by SA-RNAi is very mild. A) ChIP-Seq on sorted CNS nuclei from wor-gal4 UAS-nls-dsRed>+ and wor-gal4 UAS-nls-dsRed >cutRNAi shows a peak of H3K27Ac over the *SA* gene that disappears on *cut* knockdown. **B)** qPCR on nuclear RNA from sorted wor> nls-dsRed and wor>nls-dsRed cutRNAi nuclei shows a decrease in *SA* RNA levels. Previous studies show that cohesin can be depleted by 80-90% without affecting chromosome segregation (Dorsett, 2016). **C)** We tested for widespread effects of *SA* and nipped RNAi on NB proliferation by looking at pH3 staining at stage 13/14 and on initial NB specification by counting Dpn positive cells **(D)** in stage 13/14. Neither of these are altered. **E)** wor>SA RNAi and wor>nipped RNAi do not significantly alter Cut protein levels in NBs. **A-C)** *SA* knockdown by wor>SA RNAi results in a significant but very slight (25%) knockdown of *SA* protein levels in the VNC. It has been noted previously that *SA* is resistant to RNAi knockdown (Rollins et al., 2004) .

Table S1 Peaks with significant enrichment (p<0.001) from H3K27me3 ChIP of CNS-enriched chromatin. Unique and common peaks are shown. unique_peak1 are unique to wor>+, and unique_peak2 are unique to wor>cutRNAi.

Click here to Download Table S1

Table S2 Peaks with significant enrichment (p<0.001) from H3K27ac ChIP of CNS-enriched chromatin. Unique and common peaks are shown. unique_peak1 are unique to wor>+, and unique_peak2 are unique to wor>cutRNAi.

Click here to Download Table S2